RSC Advances

ROYAL SOCIETY
OF CHEMISTRY

www.rsc.org/advances

Graphical abstract
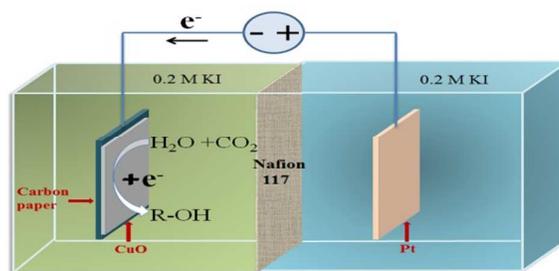
Morphology-controlled CuO nanoparticles for electroreduction of CO_2 with an excellent selectivity for ethanol.

RSC Advances

COMMUNICATION

Morphology-controlled CuO nanoparticles for electroreduction of CO$_2$ to ethanol

Dinghui Chi, Hengpan Yang, Yanfang Du, Ting Lv, Guojiao Sui, Huan Wang*, Jiaxing Lu**

CuO nanoparticles with five morphologies were synthesized in large quantities using simple method. They were *in situ* reduced to metallic Cu for the electroreduction of CO$_2$. Alcohols with excellent selectivity for ethanol were obtained. Specific morphology was demonstrated to be more electrocatalytic active than others by multiple methods.

Electrocatalytic reduction of CO$_2$ draws growing attention since it could both fix greenhouse gas and produce diverse useful compounds.[1-3] In the past years, most metals, such as Cu, Ni, Ag, Pt, Fe and Ti,[4] have been explored as cathode material for electroreduction of CO$_2$, but only Cu-based catalysts can produce hydrocarbons or alcohols with high Faradaic efficiency.[5-7] Because copper electrode has low stability especially in aqueous solutions,[8] surface modified electrodes[9-13] were utilized to get more stable and effective electrode surface. And it is also reported that the pre-[14, 15] or *in situ*[16] reduction of copper oxide was an alternative route to achieve metallic Cu for CO$_2$ reduction.

However, these Cu-based electrodes have poor selectivity, and large range of reductive products including methane, ethane, alcohols, CO and formic acid with various Faradaic efficiencies were obtained.[9-14] So it is necessary to improve the selectivity of electrodes for valuable products instead of less valuable products such as formic acid. What's more, different preparation methods for Cu-based electrodes could get different surface structures and morphologies, which would generate different electrocatalytic activity.[12-16] Therefore, the influence of surface structures and morphologies also need further exploration.

In our recent research, large quantities of CuO nanoparticles with five kinds of morphologies were synthesized by hydrothermal method (ESI†). They were directly loaded on carbon paper electrode and *in situ* reduced to metallic Cu for the electroreduction of CO$_2$. Low-carbon alcohols were obtained with excellent selectivity for ethanol, which could be used for long term chemical storage of electric energy. Moreover, it was demonstrated by multiple methods that CuO nanoparticles with different morphologies did have different electrocatalytic activity.

Firstly, CuO nanoparticles were characterized by X-Ray Diffraction. Fig. 1 clearly shows that typical diffraction peaks of CuO are contained in all the five samples, and there is no trace of other substance except for CuO, such as Cu$_2$O or Cu.
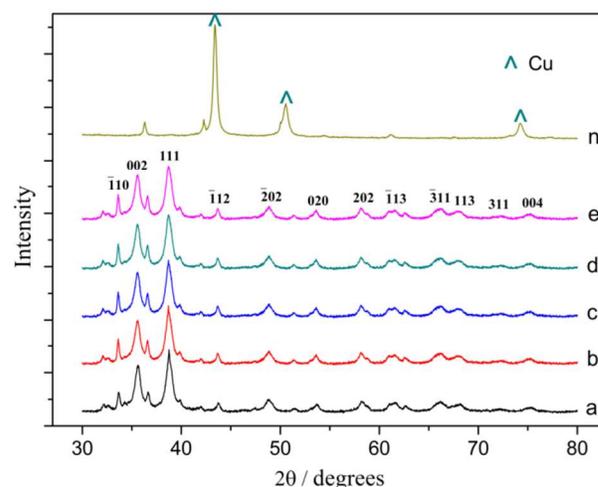
Fig.1 a-e: X-ray diffraction (XRD) patterns of CuO nanoparticles before electrolysis of sample a-e, n: sample a after 1 h electrolysis.

High-resolution SEM further characterized the structures and morphologies of CuO nanoparticles prepared under different conditions (Fig. 2). As expected, different structures and morphologies were obtained under different preparation conditions. Sample a has 3 dimensional spherical structure in the ~4 μm size range, assembled from uniform nanorods in the ~10 nm size range (Fig. 2a-1, 2a-2). Sample b also has 3

dimensional spherical structure but in the ~2µm size range, assembled from nonuniform nanoparticles in the ~200 nm size range (Fig. 2b). Sample c owns 2 dimensional structure assembled from nanoparticles in the ~200 nm size range for width and in the ~400 nm size range for length (Fig. 2c). Sample d owns nanosheet structure in the ~1µm size range for length and 400 nm for width (Fig. 2d). Sample e has uniform nanorods structure in the ~150 nm size range for length and 20 nm for width (Fig. 2e). More SEM patterns with various magnifications could be seen in Fig. S1 (ESI†).
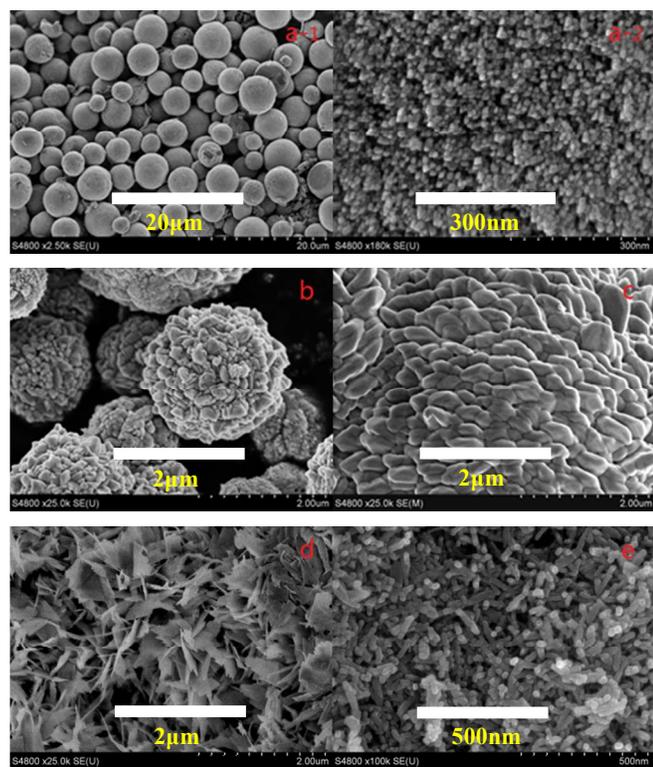
Fig. 2 FE-SEM patterns of CuO nanoparticles. (a-1), (a-2): sample a; (b)-(e): sample b-e.

In order to investigate the influence of CuO nanoparticles on CO_2 electroreduction, all the five samples with totally different structures and morphologies were loaded on carbon paper cathode for the electrolysis at a constant cathodic potential of -1.7 V in 0.2 M KI aqueous solution. In all cases, methanol (trace), ethanol and n-propanol were obtained and ethanol accounted for a proportion more than 95% (Fig. 3), which indicates that the CuO nanoparticles we synthesized have an excellent selectivity for ethanol, while mixed reduction products were achieved at Cu-based electrodes reported in previous literature.[9-14] What's more, under the same reaction conditions, sample a has obvious advantage over others, and the total Faradaic efficiencies obtained at sample a is 1.9, 2.4, 2.8 and 3.9 times more than sample b, sample c, sample d and sample e, respectively (Fig. 3A).

Nitrogen adsorption-desorption isotherms were performed to explain the different Faradaic efficiencies. Sample a has an average specific surface area of 45.4 m^2/g, which is higher than

sample b of 28.5 m^2/g, sample c of 27.1 m^2/g, sample d of 24.6 m^2/g and sample e of 25.4 m^2/g. Due to the same loaded weight and different specific surface area, this could partially be attributed to the highest surface area of sample a. However, higher surface area is not in perfect accordance with the improved Faradaic efficiency. For example, the Faradaic efficiency is 3.9 times higher on sample a than on sample e at -1.7 V in 0.2 M KI aqueous solution, but the surface area increases only 1.8 times. It was reported by other workers that morphologies of Cu-based electrodes could affect the electrocatalytic activity.[15, 17] According to SEM patterns, entirely different structures and morphologies were observed at the five samples. Therefore, the distinct morphologies of five samples would account for the difference in Faradaic efficiency as well.
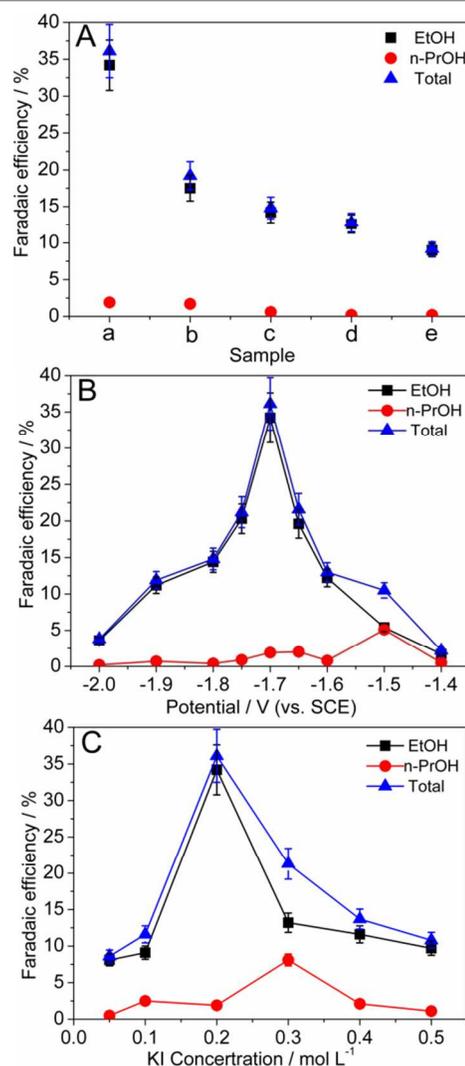
Fig. 3 Electroreduction of CO_2 under multiple conditions. A: effect of different electrodes (sample a-e), -1.7 V, 0.2 M KI; B: effect of potential, 0.2 M KI; C: effect of KI concentration, -1.7 V.

The influence of cathodic potential and electrolyte concentration were also studied. According to Fig. 3B, cathode potential has significant influence on the total Faradaic

efficiency. As cathode potential decreases from -1.4 V to -2.0 V, the total Faradaic efficiency increases first, reaching a maximum of 36.1% at -1.7 V, and decreases to 3.8% at -2.0 V. The total current density increases with the decline of potential, but the effective current density for EtOH gets a maximum at -1.7 V (Fig. S3, ESI†). As for the influence of KI concentration, a maximum of total Faradaic efficiency was obtained at 0.2 M (Fig. 3C). As contrast, 15.5% and 18.4% Faradaic efficiency for ethanol, 3.6% and 2.9% for n-propanol were obtained in 0.2 M $KHCO_3$ and $NaHCO_3$ aqueous solutions at -1.7 V, respectively. It indicated that halide ion could improve the Faradaic efficiency and selectivity of reduction products, which are consistent with those reported by other workers.[18]

The electrocatalytic activity of five samples was studied by multiple methods. Fig. 4 presents the cyclic voltammograms recorded at five samples of CuO nanoparticles from -0.4 V to -2.0 V in CO_2-saturated 0.2 M KI aqueous solutions at a scan rate of 0.1 V/s. According to these patterns, the cyclic voltammograms for all the five samples show two reductive peaks before -1.4 V, which belong to the reduction of CuO nanoparticles to metallic Cu. The generation of metallic Cu could be confirmed by XRD patterns of sample a after 1 h electrolysis. As shown in Fig. 1n, three narrow, obvious crystalline peaks correspond to metallic Cu were observed, indicating that the CuO synthesized by hydrothermal method would be *in situ* electroreduced to metallic Cu during the electrolysis process and serving as efficaciously catalysts for the formation of low-carbon alcohols.[14, 16] Sample b to e could also *in situ* generate metallic Cu during the electroreduction of CO_2 (Fig. S2, ESI†).
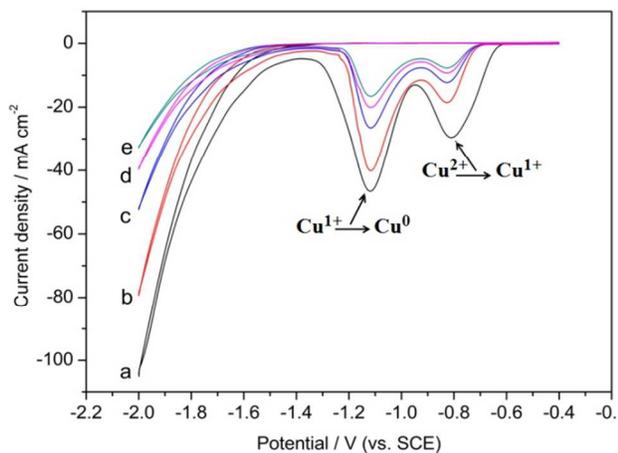
Fig. 4 Cyclic voltammograms recorded at sample a-e in CO_2-saturated 0.2M KI aqueous solution at a sweep rate of 0.1 V/s at 25°C.

And there are two higher reductive peaks in the cyclic voltammograms of sample a (Fig. 4a) than sample b to e (Fig. 4b, c, d, e), which means sample a could *in situ* generate much more metallic Cu. What's more, cathode loaded with sample a results in the most positive onset potential for CO_2 electroreduction. Moreover, the potentials due to CO_2 electroreduction at a constant current density of 10 mA cm^{-2} are used, which are -1.49 V, -1.54 V, -1.60 V, -1.62 V and -

1.64 V for sample a to e, respectively. Hence, we can infer that sample a is more electrocatalytic active than the other four for the electroreduction of CO_2.[16]

The stability of sample a to e was tested at -1.7 V in 0.2 M KI aqueous solution, all samples could remain highly active after 5 h of electrolysis. And sample a shows much higher current density during the whole test time (Fig. S4, ESI†).

In conclusion, CuO nanoparticles with high specific surface area and five morphologies were synthesized in large quantities by simple methods. They were *in situ* electroreduced to metallic Cu for the electroreduction of CO_2. It was demonstrated by multiple methods that structures and morphologies of CuO nanoparticles did have great influence on electrocatalytic activity.

Notes and references

Shanghai Key Laboratory of Green Chemistry and Chemical Processes, Department of Chemistry, East China Normal University, Shanghai 200062, China.

*Corresponding Author: Dr. Huan Wang (Tel: +8621-52134935, E-mail: hwang@chem.ecnu.edu.cn).

**Corresponding Author: Prof. Jia-Xing Lu (Tel: +8621-62233491, E-mail: jxlu@chem.ecnu.edu.cn).

† Electronic Supplementary Information (ESI) available: materials, instruments, general methods, characterization of CuO nanoparticles. See DOI: 10.1039/c000000x/

1. Y. Eds., The Electrochemical Society: Pennington, NJ, 1993, p1.
2. M. Gattrell, N. Gupta, A. Co, *J. Electroanal. Chem.,* 2006, **594**, 1-19.
3. M. Le, M. Ren, Z. Zhang, P.T. Spunger, R.L. Kurtz, J.C. Flake, *J. Electrochem. Soc.,* 2011, **158**, E45-E49.
4. J.L. Qiao, Y.Y. Liu, F. Hong, J.J. Zhang, *Chem. Soc. Rev.,* 2014, **43**, 631-675.
5. Y. Hori, R. Takahashi, Y. Yoshinami, A, Murata, J. Phys. Chem. B, 1997, **101**,7075-7081
6. Y. Hori, K. Kikuchi, A. Murata, S. Suzuki, *Chem. Lett.,* 1986, **6**, 897-898.
7. K. Hara, A. Tsuneto, A. Kudo, T. Sakata, *J. Electrochem. Soc.,* 1994, **141**, 2097-2103.
8. Y. Hori, Modern Aspects of Electrochemistry, Springer, New York, 2008. 89-189.
9. K. Ogura, H. Yano, F. Shirai, *J. Electrochem. Soc.,* 2003, **150**, D163-D168.
10. H. Yano, T. Tanaka, M. Nakayama, K. Ogura, *J. Electroanal. Chem.,* 2004, **565**, 287-293.
11. K. Ogura, R. Oohara, Y. Kudo, *J. Electrochem. Soc.,* 2005, **152**, D213-D219.
12. M.R. Goncalves, A. Gomes, J. Condeco, T.R.C. Fernandes, T. Pardal, C.A.C. Sequeira, J.B. Branco, *Electrochim. Acta,* 2013, **102**, 388-392.
13. M.R. Goncalves, A. Gomes, J. Condeco, R. Fernandes, T. Pardal, C.A.C. Sequeira, J.B. Branco, *Energy Convers. Manag.,* 2010, **51**, 30-32.
14. C.W. Li, M.W. Kanan, *J. Am. Chem. Soc.,* 2012, **134**, 7231-7234.
15. J.L. Qiao, P. Jiang, J.S. Liu, J.J. Zhang, *Electrochem. Commun.,* 2014, **38**, 8-11.
16. C.W. Li, J. Ciston, M.W. Kanan, *Nature,* 2014, **508**, 504-507.
17. W. Tang, A.A. Peterson, A.S. Varela, Z.P. Jovanov, L. Bech, W.J. Durand, S. Dahl, J.K. Nørskov, I. Chorkendorff, *Phys. Chem. Chem. Phys.,* 2012, **14**, 76-81.
18. H. Yano, T. Tanaka, M. Nakayama, K. Ogura, *J. Electrochem. Soc.,* 2004, **565**, 287-293.